doi:10.1038/nature11019

ZNRF3 promotes Wnt receptor turnover in an R-spondin-sensitive manner

Huai-Xiang Hao[1]*, Yang Xie[1]*, Yue Zhang[1]†, Olga Charlat[1], Emma Oster[1], Monika Avello[1], Hong Lei[1], Craig Mickanin[1], Dong Liu[1], Heinz Ruffner[2], Xiaohong Mao[1], Qicheng Ma[1], Raffaella Zamponi[1], Tewis Bouwmeester[2], Peter M. Finan[1], Marc W. Kirschner[3], Jeffery A. Porter[1], Fabrizio C. Serluca[1] & Feng Cong[1]

R-spondin proteins strongly potentiate Wnt signalling and function as stem-cell growth factors. Despite the biological and therapeutic significance, the molecular mechanism of R-spondin action remains unclear. Here we show that the cell-surface transmembrane E3 ubiquitin ligase zinc and ring finger 3 (ZNRF3) and its homologue ring finger 43 (RNF43) are negative feedback regulators of Wnt signalling. ZNRF3 is associated with the Wnt receptor complex, and inhibits Wnt signalling by promoting the turnover of frizzled and LRP6. Inhibition of ZNRF3 enhances Wnt/β-catenin signalling and disrupts Wnt/planar cell polarity signalling *in vivo*. Notably, R-spondin mimics ZNRF3 inhibition by increasing the membrane level of Wnt receptors. Mechanistically, R-spondin interacts with the extracellular domain of ZNRF3 and induces the association between ZNRF3 and LGR4, which results in membrane clearance of ZNRF3. These data suggest that R-spondin enhances Wnt signalling by inhibiting ZNRF3. Our study provides new mechanistic insights into the regulation of Wnt receptor turnover, and reveals ZNRF3 as a tractable target for therapeutic exploration.

Wnt proteins regulate the turnover of the transcription cofactor β-catenin and control key developmental gene expression programs[1,2]. Wnt proteins also induce planar cell polarity (PCP) or tissue polarity signalling, which governs cell and tissue movements[3]. Various secreted Wnt modulators and several feedback control mechanisms help to determine the proper signalling output. Perturbation of Wnt signalling can lead to degenerative diseases and cancer.

R-spondin proteins (RSPO1–4) strongly potentiate Wnt/β-catenin signalling and Wnt/PCP signalling[4–7] and regulate tissue patterning and differentiation[4,8–11]. R-spondin proteins are potent stem-cell growth factors[12]. RSPO1 strongly stimulates the proliferation of crypt stem cells[5,13] and protects mice from chemotherapy-induced mucositis[14]. Despite the biological and therapeutic significance, the mechanism of R-spondin action is unclear[4,7,15–17]. Recently, several groups including ours have demonstrated that the stem-cell marker LGR5 and its homologue LGR4 are R-spondin receptors essential for R-spondin-induced β-catenin and PCP signalling[18–20] (H.R. *et al.*, manuscript submitted). However, the mechanism by which R-spondin and LGR4 and LGR5 potentiate Wnt signalling remains unknown.

Here we identify the transmembrane E3 ubiquitin ligase ZNRF3 as the molecular target of R-spondin. Our data suggest that ZNRF3 inhibits Wnt signalling by promoting the turnover of frizzled and LRP6, and its activity is inhibited by R-spondin. Our study uncovers a new mechanism that controls Wnt receptor turnover, and its therapeutic exploration holds promise in regenerative medicine.

ZNRF3 as a negative regulator of Wnt pathway

Many negative regulators of Wnt/β-catenin signalling (for example, AXIN2) are β-catenin target genes and function in negative feedback loops. To identify new β-catenin target genes and potential negative regulators of Wnt signalling, primary tissue microarray data (NCBI accession GEO2109) were analysed for genes in which messenger RNA expression is positively correlated with *AXIN2* mRNA. This analysis identified *ZNRF3* and *RNF43* as β-catenin target genes. The expression of *ZNRF3* and *RNF43* was induced by Wnt3a conditioned media (Supplementary Fig. 1a). The expression of both genes was increased in primary colorectal tumours exhibiting hyperactive β-catenin signalling (Supplementary Fig. 1b). Furthermore, *ZNRF3* mRNA expression in the SW480 colorectal cancer cell line was down-regulated by β-catenin short interfering RNA (siRNA; Supplementary Fig. 1c).

ZNRF3 and RNF43 are highly related RING finger proteins (Supplementary Fig. 2). Both proteins contain a signal peptide, an extracellular domain, a transmembrane domain and an intracellular RING domain (Fig. 1a and Supplementary Fig. 2). ZNRF3 conjugated to green fluorescent protein (ZNRF3–GFP) is localized to the plasma membrane, whereas ZNRF3–GFP lacking the signal peptide (ZNRF3 ΔSP–GFP) is predominantly cytoplasmic (Supplementary Fig. 3a). These results were confirmed using a cell-surface protein biotinylation assay (Supplementary Fig. 3b). RNF43–GFP is also localized to the plasma membrane (data now shown). Furthermore, the intracellular fragment of ZNRF3 showed RING domain-dependent autoubiquitylation in an *in vitro* ubiquitylation assay (Supplementary Fig. 3c). These results suggest that ZNRF3 and RNF43 are E3 ubiquitin ligases localized to the plasma membrane.

We tested the function of ZNRF3 and RNF43 in Wnt/β-catenin signalling using HEK293 cells transfected with the Super-Topflash (STF) luciferase reporter. Depletion of ZNRF3, but not RNF43, strongly increased STF activity in the absence or presence of exogenous Wnt3a (Fig. 1b and Supplementary Fig. 4a). Overexpression of siRNA-resistant *ZNRF3* completely abolished *ZNRF3* siRNA-induced STF activation, suggesting that the effect of *ZNRF3* siRNA is on-target (Fig. 1c). In addition, the overexpression of wild-type ZNRF3 decreased Wnt3a-induced STF activation, whereas the overexpression of a ZNRF3 mutant lacking the RING domain (ZNRF3 ΔRING) strongly increased STF activity (Fig. 1c), indicating a

[1]Novartis Institutes for Biomedical Research, 250 Massachusetts Avenue, Cambridge, Massachusetts 02139, USA. [2]Novartis Institutes for Biomedical Research, Novartis Pharma AG, Postfach CH-4002 Basel, Switzerland. [3]Department of Systems Biology, Harvard Medical School, Boston, Massachusetts 02115, USA. †Present address: AstraZeneca, 35 Gatehouse Drive, Waltham, Massachusetts 02451, USA.
*These authors contributed equally to this work.

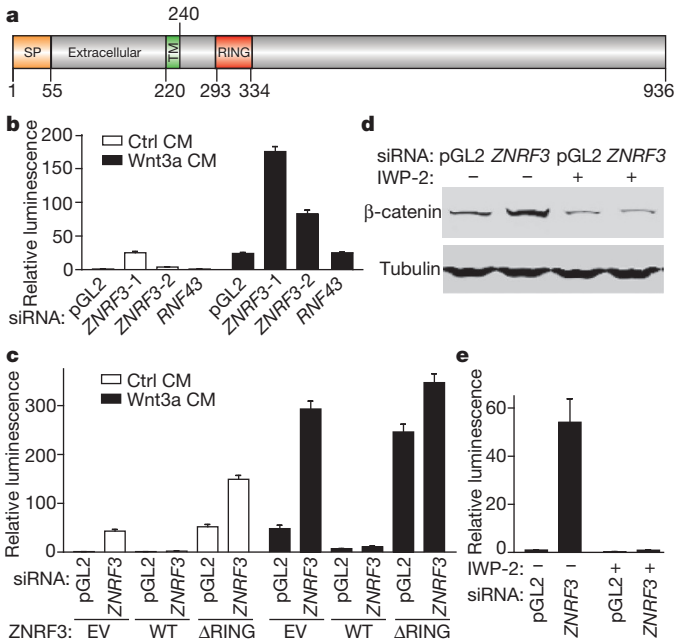

Figure 1 | ZNRF3 negatively modulates Wnt signalling. **a**, A schematic diagram of the domain structure of ZNRF3. SP, signal peptide; TM, transmembrane domain. **b**, Depletion of ZNRF3 increases the activity of the STF reporter in HEK293 cells. pGL2 siRNA acts as a negative control. CM, conditioned media; ctrl, control. **c**, *ZNRF3* siRNA-induced activation of STF is inhibited by siRNA-resistant *ZNRF3*, and ZNRF3 ΔRING increases STF activity. EV, empty vector; WT, wild type. **d**, *ZNRF3* siRNA-induced stabilization of cytoslic β-catenin is inhibited by the porcupine inhibitor IWP-2 (1 μM). **e**, STF reporter assay of HEK293 STF cells treated as in **d**. Error bars denote s.d.; $n = 4$ (**b**, **c**, **e**).

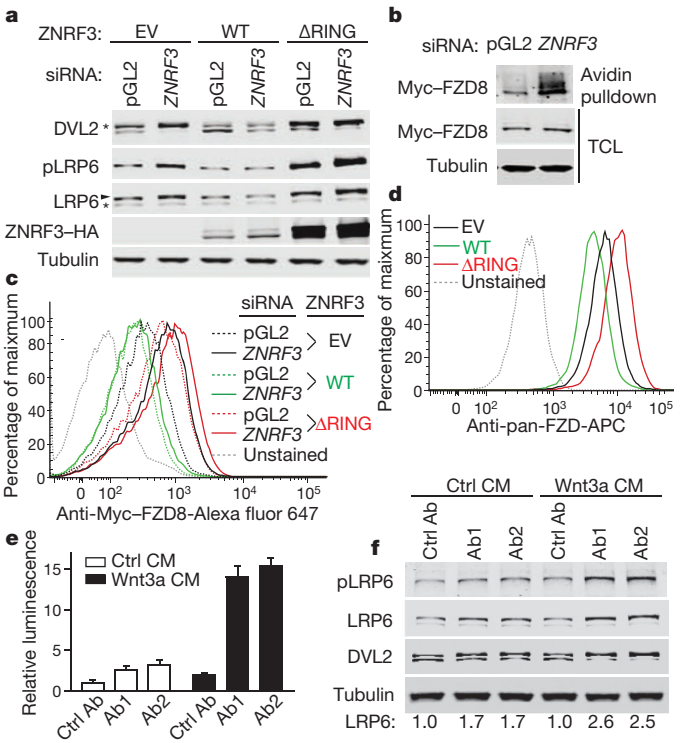

Figure 2 | ZNRF3 regulates the level of Wnt receptors on the cell surface. **a**, *ZNRF3* siRNA and ZNRF3 ΔRING increase the level of LRP6 and phosphorylated DVL2. The upper band of DVL2, indicated by an asterisk, is the phosphorylated form, and the lower band is the non-phosphorylated form. The mature and the ER form of LRP6 are indicated by an arrowhead and asterisk, respectively. pLRP6, phosphorylated LRP6. **b**, Depletion of ZNRF3 increases the cell-surface level of Myc–FZD8. TCL, total cell lysates. **c**, Flow cytometric analysis of membrane Myc–FZD8 in cells transfected with the indicated vector and siRNA. **d**, Overexpression of ZNRF3 decreases, and overexpression of ZNRF3 ΔRING increases, the cell-surface level of endogenous frizzled proteins. APC, allophycocyanin. **e**, ZNRF3 antagonistic antibodies (Ab1 and Ab2; 50 μg ml^{-1}) increase STF activity in HEK293 cells. Error bars denote s.d., $n = 4$. **f**, Immunoblots of indicated proteins for the same cells and treatments as described in **e**. Bottom, densitometric quantification of LRP6.

dominant-negative function of ZNRF3 ΔRING. Similarly, the overexpression of wild-type RNF43 blocked *ZNRF3*-siRNA-induced STF activation, whereas overexpression of RNF43 ΔRING increased STF activity (Supplementary Fig. 4b). These results indicate that ZNRF3 and RNF43 are functional homologues that act as negative regulators of Wnt/β-catenin signalling. On the basis of the threshold cycle (C_t) values observed in a quantitative PCR assay, *ZNRF3* is the dominantly expressed homologue in HEK293 cells (Supplementary Fig. 4a). Furthermore, IWP-2—a porcupine inhibitor that blocks Wnt secretion[21]—completely inhibited β-catenin accumulation and STF activation induced by *ZNRF3* siRNA or ZNRF3 ΔRING (Fig. 1d, e and data not shown) in the absence of exogenous Wnt3a. This result suggests that ZNRF3 suppresses the β-catenin signalling initiated by endogenous Wnt proteins, and this distinguishes ZNRF3 from other negative regulators of Wnt signalling such as adenomatous polyposis coli (APC), AXIN1/2 and glycogen synthase kinase 3-α/β (GSK3-α/β).

ZNRF3 regulates the stability of LRP6 and frizzled

Biochemical experiments were carried out to determine the molecular mechanism by which ZNRF3 regulates β-catenin signalling. Treatment with *ZNRF3* siRNA or overexpression of ZNRF3 ΔRING increased the levels of phosphorylated LRP6 and total LRP6 (Fig. 2a), and the effect of *ZNRF3* siRNA is blocked by the expression of siRNA-resistant *ZNRF3* (Fig. 2a). Increased LRP6 plasma membrane expression after ZNRF3 inhibition was confirmed using flow cytometry (Supplementary Fig. 5a).

Notably, treatment with *ZNRF3* siRNA or overexpression of ZNRF3 ΔRING increased the phosphorylation of dishevelled-2 (DVL2) (Fig. 2a), whereas DVL2 phosphorylation was decreased by ZNRF3 overexpression (Fig. 2a). As dishevelled phosphorylation is a direct readout of frizzled activation and is independent of LRP6 activation[22], these results suggest that the level or activity of frizzled might also be affected by ZNRF3. To test this hypothesis, HEK293 cells stably expressing amino-terminal Myc-tagged frizzled 8 (FZD8) were generated. In these cells, most Myc–FZD8 is trapped in the endoplasmic reticulum (ER), and only a small fraction is localized to the plasma membrane (data not shown). A cell-surface protein biotinylation assay showed that *ZNRF3* siRNA strongly increased the level of Myc–FZD8 on the plasma membrane without affecting the level of total Myc–FZD8 (Fig. 2b). Furthermore, *ZNRF3* siRNA and ZNRF3 ΔRING increased, whereas ZNRF3 decreased, the membrane level of Myc-FZD8 as determined by flow cytometry (Fig. 2c). Using pan-frizzled antibody 18R5 (ref. 23), the cell-surface level of endogenous frizzled proteins was found to be decreased or increased after the overexpression of ZNRF3 or ZNRF3 ΔRING, respectively (Fig. 2d). Inhibition of ZNRF3 also resulted in increased membrane levels of Myc–FZD4 (Fig. 3c), Myc–FZD5 (Supplementary Fig. 5b) and endogenous FZD6 (Supplementary Fig. 5c). Taken together, these results suggest that ZNRF3 regulates the membrane levels of frizzled and LRP6.

Because ZNRF3 is localized to the plasma membrane, antagonism of ZNRF3 using an antibody-based approach was explored. Two antibodies targeting the extracellular domain of ZNRF3 were identified that phenocopied *ZNRF3* siRNA treatment. Both antibodies enhanced Wnt3a-induced STF activity (Fig. 2e) and modestly increased the level of LRP6 (Fig. 2f) or membrane Myc–FZD8 (Supplementary Fig. 5d). These results further strengthen the conclusion that ZNRF3 inhibits Wnt signalling by decreasing the membrane levels of frizzled and LRP6.

Next we tested whether ZNRF3 inhibition affects the stability of LRP6 and Myc–FZD8. Overexpression of ZNRF3 ΔRING extended the half-life of LRP6 or membrane Myc–FZD8 in a ^{35}S-labelling-based or a cell-surface protein biotinylation-based pulse-chase experiment (Fig. 3a, b). These results suggest that ZNRF3 promotes the degradation of LRP6 and frizzled. Multiubiquitylation of frizzled promotes its lysosomal targeting and degradation[24]. We tested whether ZNRF3 is responsible for frizzled ubiquitylation. Myc-tagged FZD4 was used for this study because of its higher membrane expression level. Consistent with a previous report[24], FZD4 K0—in which all intracellular Lys residues are mutated to Ala—was expressed at a much higher level than wild-type FZD4 at the plasma membrane (Fig. 3c). Depletion of ZNRF3 increased the membrane level of wild-type FZD4, but not FZD4 K0 (Fig. 3c). Importantly, the overexpression of ZNRF3 ΔRING or depletion of endogenous ZNRF3 suppressed the ubiquitylation of FZD4 (Fig. 3d and Supplementary Fig. 5e), whereas the overexpression of ZNRF3 increased ubiquitylation of FZD4 (Supplementary Fig. 5f). Together, these results suggest that ZNRF3 promotes the degradation of frizzled by increasing its ubiquitylation.

Regulation of frizzled and LRP6 by ZNRF3 raises the possibility that ZNRF3 exists in the same complex as frizzled and LRP6. Indeed, co-expressed haemagglutinin-tagged ZNRF3 (ZNRF3–HA) and Myc–FZD8 can be co-immunoprecipitated (Fig. 3e). Furthermore, stably expressed ZNRF3–HA can be co-immunoprecipitated with endogenous LRP6 or FZD6 but not with other membrane proteins such as epidermal growth factor receptor (EGFR) and insulin receptor-β (IR-β) (Fig. 3f and Supplementary Fig. 6). Together, these results suggest that ZNRF3 exists in the same complex with frizzled and LRP6 and promotes their turnover.

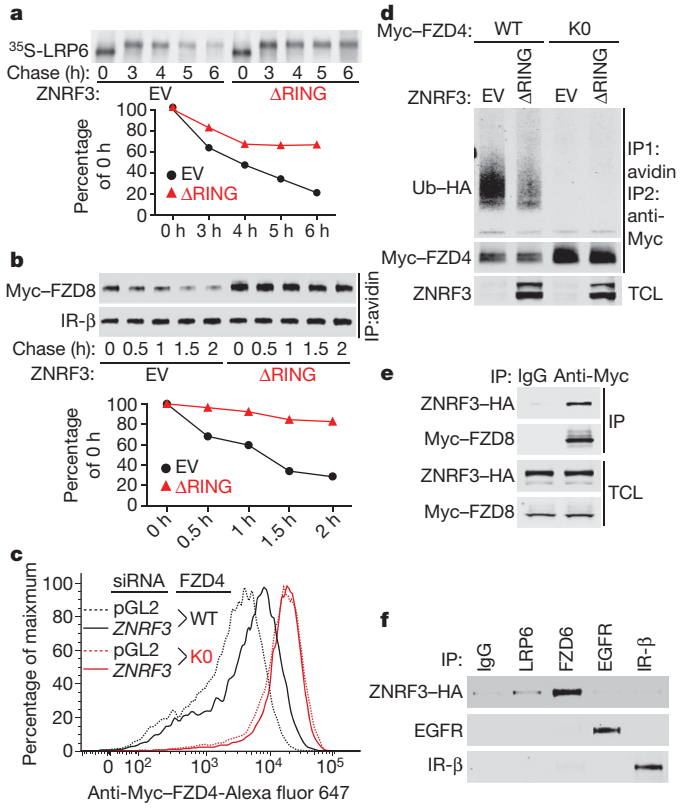

Figure 3 | ZNRF3 regulates the stability of LRP6 and frizzled through ubiquitylation. **a**, ZNRF3 ΔRING extends the half-life of LRP6 in a radioactive pulse chase assay. Bottom, densitometric quantification. **b**, ZNRF3 ΔRING extends the half-life of Myc–FZD8 in a surface protein biotinylation-based pulse chase assay. Insulin receptor-β (IR-β) acts as a control. Bottom, densitometric quantification of Myc–FZD8. IP, immunoprecipitate. **c**, ZNRF3 ΔRING increases the membrane level of Myc–FZD4 but not that of the K0 mutant. **d**, ZNRF3 ΔRING decreases ubiquitylation (Ub) of Myc–FZD4. **e**, Co-immunoprecipitation of Myc–FZD8 and ZNRF3–HA. **f**, Co-immunoprecipitation of ZNRF3–HA with endogenous LRP6 and FZD6. EGFR and IR-β act as negative controls.

R-spondin stabilizes Wnt receptors by suppressing ZNRF3

R-spondin potentiates Wnt/β-catenin and Wnt/PCP signalling through an unknown mechanism. Because frizzled is shared by Wnt/β-catenin and Wnt/PCP pathways and R-spondin induces dishevelled phosphorylation[16], we proposed that R-spondin might potentiate Wnt signalling by increasing the membrane level of frizzled proteins. Indeed, RSPO1 increased the membrane level of Myc–FZD8 (Fig. 4a and Supplementary Fig. 7a), and inhibited its degradation (Supplementary Fig. 7b). RSPO1 also increased the membrane level of endogenous frizzled proteins (Fig. 4b), Myc–FZD4 (Supplementary Fig. 7c), Myc–FZD5 (Supplementary Fig. 7d) and endogenous FZD6 (Supplementary Fig. 7e). RSPO2, RSPO3 and RSPO4 also increased the membrane level of endogenous frizzled proteins (Supplementary Figs 7f). Notably, RSPO1 decreased the ubiquitylation of FZD4 (Fig. 4c). In agreement with previous findings[17], RSPO1 and RSPO2 also increased the level of mature LRP6 (Fig. 4d). Consistent with a crucial role for LGR4 in R-spondin signalling, the depletion of LGR4 (Supplementary Fig. 8a) blocked RSPO1-induced accumulation of membrane Myc–FZD8 (Supplementary Fig. 8b, c) and LRP6 (Supplementary Fig. 8d), and abolished the effect of RSPO1 on FZD4 ubiquitylation (Supplementary Fig. 8e). Because ZNRF3 is required for frizzled ubiquitylation and R-spondin mimics *ZNRF3* siRNA in several assays, R-spondin might function by inhibiting ZNRF3. Indeed, RSPO1 did not increase STF activity in cells overexpressing ZNRF3 ΔRING (Supplementary Fig. 9a). In addition, RSPO1 did not further increase, and *LGR4* siRNA did not decrease, the membrane accumulation of Myc–FZD8 induced by ZNRF3 inhibition (Supplementary Fig. 9b, c). These results suggest that ZNRF3 functions downstream of R-spondin and LGR4.

Conservation of the extracellular domains (ECD) of ZNRF3 and RNF43 (Supplementary Fig. 2) and identification of ZNRF3 antagonistic antibodies indicate the existence of ligands for these proteins. Because R-spondin functionally mimics *ZNRF3* siRNA, the possibility that R-spondin directly interacts with ZNRF3 ECD was considered. Interestingly, RSPO1–GFP bound to cells overexpressing ZNRF3 ECD-TM, which lacks most of the intracellular domain, but did not bind to cells overexpressing FZD4 (Fig. 4e). This binding does not require endogenous LGR4 (Supplementary Fig. 10a). In a solution-based binding assay, RSPO1–GFP was copurified with ZNRF3 ECD–Fc, but not with FZD8 CRD (cysteine-rich domain)-Fc (Fig. 4f). As a control, Wnt3a was copurified with FZD8 CRD–Fc, but not with ZNRF3 ECD–Fc (Supplementary Fig. 10b). Furthermore, the mutation of ZNRF3 ECD Pro 103 to Ala severely disrupted its binding to RSPO1 in cell-based and solution-based binding assays (Fig. 4e, f). Together, these results indicate that R-spondin specifically interacts with the extracellular domain of ZNRF3.

If R-spondin increases Wnt signalling by binding to ZNRF3, the overexpression of ZNRF3 ECD might inhibit R-spondin-mediated signalling. We found that the overexpression of ZNRF3 ECD-TM completely blocked RSPO1-induced, but not Wnt3a-induced, STF activation and β-catenin stabilization (Fig. 4g, h), whereas ZNRF3 ECD-TM P103A had a much weaker effect (Supplementary Fig. 10c). Notably, the overexpression of ZNRF3 ECD-TM completely blocked RSPO1-induced membrane accumulation of frizzled proteins (Supplementary Fig. 10d). These results suggest that ZNRF3 ECD-TM inhibits R-spondin signalling, probably by functioning as a pseudoreceptor.

Because R-spondin binds to both LGR4 and ZNRF3, it might induce the association between the two proteins. Treatment with RSPO1 increased the interaction between exogenously expressed LGR4 and ZNRF3 in a coimmunoprecipitation assay (Fig. 5a). RSPO1 markedly

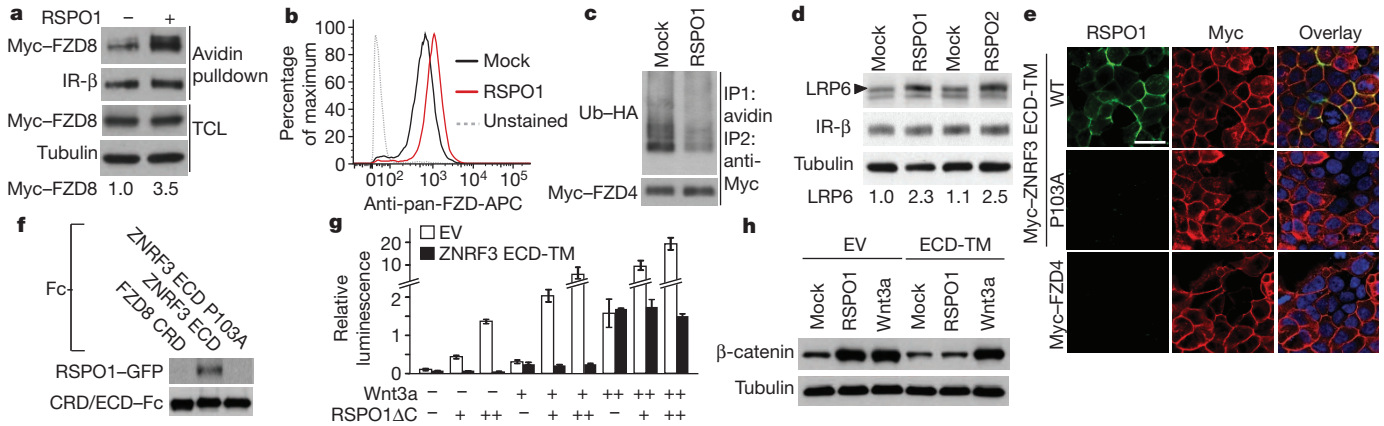

Figure 4 | RSPO1 increases the cell-surface level of frizzled proteins and functionally interacts with the extracellular domain of ZNRF3. **a**, RSPO1 (200 ng ml^{-1}) increases the membrane level of Myc–FZD8. Bottom, densitometric quantification. **b**, RSPO1 increases the membrane level of endogenous frizzled proteins. **c**, RSPO1 inhibits ubiquitylation of FZD4. **d**, RSPO1 and RSPO2 increase the level of LRP6. The mature form of LRP6 is indicated by an arrowhead. Bottom, densitometric quantification. **e**, RSPO1–GFP specifically interacts with overexpressed Myc-tagged ZNRF3 ECD-TM. The nuclei were stained with 4′,6-diamidino-2-phenylindole. Scale bar, 20 μm. **f**, RSPO1–GFP specifically interacts with the extracellular domain of ZNRF3. **g**, Overexpression of ZNRF3 ECD-TM specifically inhibits RSPO1-induced STF activation. RSPO1ΔC lacks 36 amino acid residues at the C terminus. Error bars denote s.d., $n = 4$. **h**, Overexpression of ZNRF3 ECD-TM specifically inhibits RSPO1-induced cytosolic β-catenin stabilization.

decreased the membrane level of ZNRF3 (Fig. 5b), but not that of ZNRF3 P103A (Supplementary Fig. 11a), in a cell-surface protein biotinylation assay. RSPO1-induced membrane clearance of ZNRF3 is LGR4-dependent (Supplementary Fig. 11b). As R-spondin induces the association between LGR4 and ZNRF3, we asked whether the forced dimerization of LGR4 and ZNRF3 would induce membrane clearance of ZNRF3. The heterodimerization domain DmrA or DmrC was fused to the carboxy terminus of ZNRF3 or LGR4, and these two chimaeric proteins were co-expressed in HEK293 cells. As seen in Fig. 5c, d, the treatment of cells with small molecule A/C dimerizer or with RSPO1 considerably reduced the membrane level of ZNRF3. Interestingly, RSPO1 and A/C dimerizer failed to decrease the membrane level of ZNRF3 ΔRING (Supplementary Fig. 11a, c), suggesting that the membrane clearance of ZNRF3 requires its E3 ligase activity. Taken together, these results suggest that R-spondin induces membrane clearance of ZNRF3 through LGR4, leading to accumulation of Wnt receptors on the cell surface.

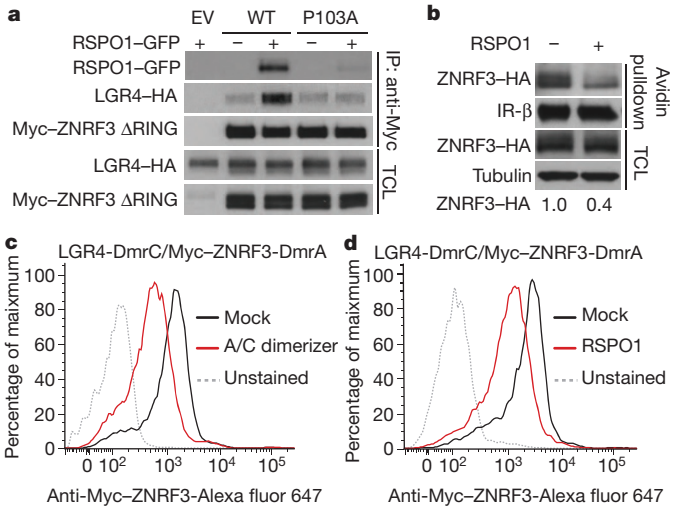

Figure 5 | RSPO1 increases the interaction between ZNRF3 and LGR4 and induces membrane clearance of ZNRF3. **a**, RSPO1 increases the interaction between ZNRF3 and LGR4. **b**, RSPO1 decreases the membrane level of ZNRF3. Bottom, densitometric quantification of cell-surface ZNRF3. **c**, **d**, Forced heterodimerization of LGR4 and ZNRF3 induces membrane clearance of ZNRF3.

ZNRF3 regulates β-catenin and PCP signalling *in vivo*

Because frizzled proteins are required for both Wnt/β-catenin and Wnt/PCP signalling, the inhibition of ZNRF3 is expected to promote both β-catenin and PCP signalling. We tested this hypothesis in various model organisms. The overexpression of human ZNRF3 ΔRING, but not wild-type ZNRF3, in zebrafish embryos resulted in the loss of anterior neural structures (Fig. 6a) and reduced expression of the anterior neural markers *hesx1* and *rx3* (Fig. 6b), consistent with ectopic activation of β-catenin signalling[25]. This phenotype was rescued by co-expression of AXIN1 (Supplementary Fig. 12a). Furthermore, the overexpression of human ZNRF3 ΔRING in *Xenopus* embryos led to axis duplication (Supplementary Fig. 12c) and increased expression of the β-catenin target gene *siamois* and *xnr3* in animal caps (Supplementary Fig. 12d). Induction of typical phenotypes associated with excessive β-catenin signalling by ZNRF3 ΔRING suggests that ZNRF3 suppresses β-catenin signalling *in vivo*. Precise regulation of PCP signalling output is required for normal gastrulation, and either increased or decreased PCP signalling disrupts convergent extension movements. The overexpression of wild-type ZNRF3 or ZNRF3 ΔRING in zebrafish embryos produced phenotypes characteristic of convergent extension defects, such as shortened body axis (Fig. 6c) and broader somites (Fig. 6d). Overexpression of wild-type ZNRF3 frequently caused axis bifurcation (Fig. 6d), and, interestingly, the same phenotype was also produced by overexpression of a dominant-negative frizzled[26]. Furthermore, the overexpression of wild-type ZNRF3 or ZNRF3 ΔRING disrupts dorsolateral cellular movements in a cell transplantation assay (Fig. 6e) and a fluorescent lineage tracing assay (Supplementary Fig. 12e). Notably, the overexpression of ZNRF3 ΔRINGΔSP (missing the signal peptide) had no effect on the expression of anterior neural markers and on convergent extension (Supplementary Fig. 12f)

To study the function of ZNRF3 in mice, *Znrf3* knockout mice were generated and backcrossed to a C57BL/6J background (Supplementary Fig. 13). *Znrf3*-deficient embryos died around birth. It is established that suppression of Wnt/β-catenin signalling in the lens placode is crucial for lens development; ectopic activation of β-catenin signalling in eyes blocks lens formation and eye-specific deletion of β-catenin leads to the formation of ectopic lentoid bodies[27–29]. The most obvious phenotype of *Znrf3* knockout embryos is the lack of lens formation (Fig. 6f and Supplementary Fig. 14a). Axin2–LacZ was negative in the lens placode of embryonic day (E)9.5 wild-type embryos, but it was positive in *Znrf3* knockout embryos (Fig. 6g). Expression of the β-catenin target gene

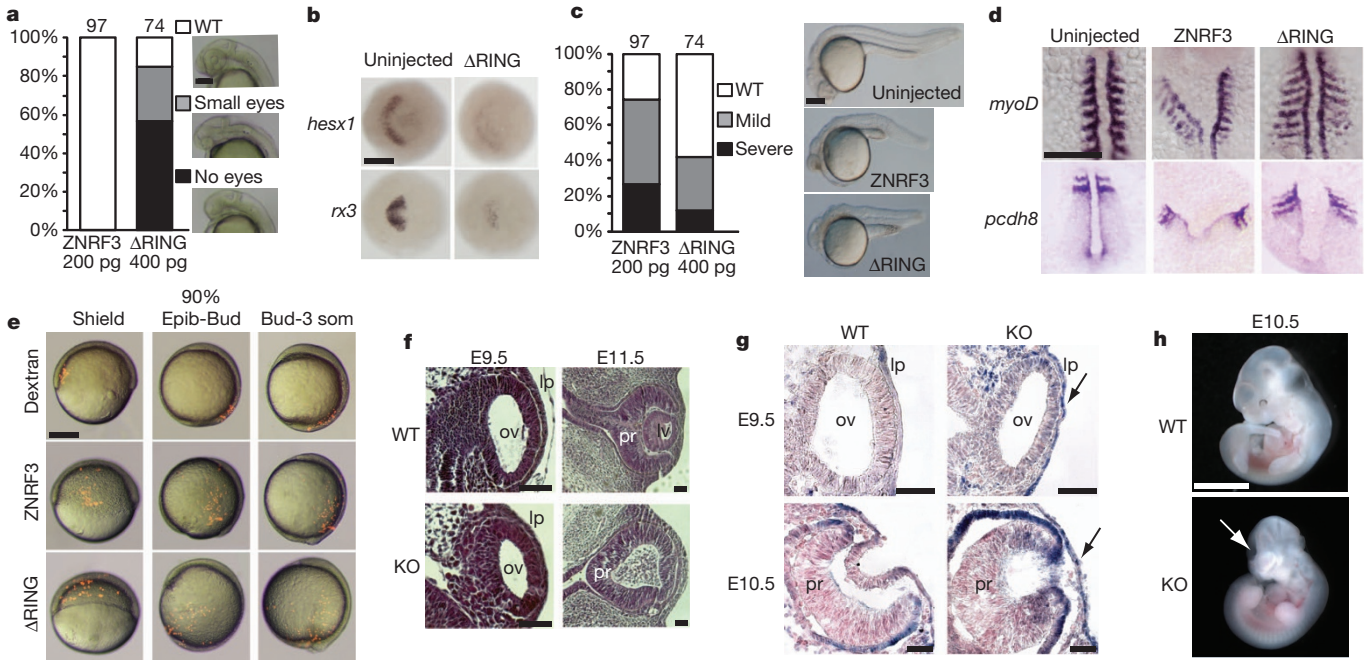

Figure 6 | ZNRF3 regulates both Wnt/β-catenin and Wnt/PCP signalling *in vivo*. **a**, Overexpression of ZNRF3 ΔRING in zebrafish embryos induces small eyes or loss of eyes, as shown in the right panel. Left, histogram of the frequency of the eye-loss phenotype. Numbers of embryos per treatment are indicated above the bars. **b**, Overexpression of ZNRF3 ΔRING in zebrafish greatly reduces the expression of anterior neural marker *hesx1* and the forebrain and retinal marker *rx3*. **c**, Overexpression of ZNRF3 or ZNRF3 ΔRING in zebrafish induces compressed somites and a shortened anterior–posterior axis. **d**, Top, *myoD* staining at the 8–9-somite stage. Zebrafish embryos injected with either mRNA have thinned and widened somites. Note that embryos injected with *ZNRF3* mRNA often display a bifurcated axis phenotype. Bottom, dorsal view of *pcdh8* expression at the 3-somite stage. **e**, Ovexpression of ZNRF3 or ZNRF3 ΔRING delays convergent extension movements. 90% Epib-Bud: 90% epiboly to tailbud stage; bud-3 som: tailbud to 3-somite stage. **f**, Haematoxylin and eosin staining of the eye region of E9.5 and E11.5 *Znrf3* wild-type (WT) and knockout (KO) mouse embryos. Lp, lens placode; lv, lens vesicle; ov, optic vesicle; pr, presumptive retina. **g**, Increased Axin2-LacZ activity in the lens placode of E9.5 and E10.5 *Znrf3* knockout mouse embryos. Arrows indicate Axin2-LacZ-positive cells. **h**, Gross morphology of E10.5 *Znrf3* wild-type and knockout mouse embryos with neural tube defects. Arrow indicates open neural tube in the *Znrf3* knockout embryo. Scale bars, 200 μm (**a**–**e**), 50 μm (**f**, **g**) and 2 mm (**h**).

Axin2 was also markedly increased in the eye region of E9.5 *Znrf3* knockout embryos (Supplementary Fig. 14b). In E10.5 *Znrf3* knockout embryos, thickening and invagination of presumptive retina is normal, but thickening and invagination of lens placode, which was associated with increased Axin2–LacZ, was completely blocked (Fig. 6g). These results are consistent with an important role of Wnt inhibition in lens development. Wnt/PCP signalling is essential for cell movements during narrowing of the folding neural plate[30]. Interestingly, about 20% of the *Znrf3* knockout embryos show neural tube closure defects (Fig. 6h and Supplementary Fig. 14a), which probably result from disrupted Wnt/PCP signalling. Taken together, these results suggest that ZNRF3 regulates both Wnt/β-catenin and Wnt/PCP signalling *in vivo*. Because RNF43 is a functional homologue of ZNRF3, the study of *Znrf3* and *Rnf43* double knockout mice should yield further information of these genes in embryonic development and adult tissue homeostasis.

Discussion

Our data support a model in which ZNRF3 and LGR4 form a receptor complex for R-spondin (Supplementary Fig. 15). In the absence of R-spondin, ZNRF3 ubiquitylates frizzled and promotes the degradation of frizzled and LRP6, leading to attenuated canonical and non-canonical Wnt signalling. When R-spondin is present, it induces the interaction between ZNRF3 and LGR4, leading to the membrane clearance of ZNRF3. This results in accumulation of frizzled and LRP6 on the plasma membrane and enhances canonical and non-canonical Wnt signalling. ZNRF3 is a unique transmembrane ubiquitin E3 ligase, the activity of which is directly regulated by ligand binding. We have demonstrated ZNRF3 as a tractable target through the identification of two ZNRF3 antagonizing antibodies. Potential application of such antibodies in regenerative medicine should be further explored.

Previously known cancer-associated Wnt pathway mutations all occur in the downstream components of the pathway, such as APC, AXIN1/2 and β-catenin. However, most Wnt inhibitors being developed at present would not inhibit Wnt signalling in tumours with downstream pathway mutations. During revision of the manuscript, RNF43 was identified as a tumour suppressor in cystic pancreatic tumours[31]. To our knowledge, RNF43 represents the first upstream Wnt pathway component mutated in cancers. This provides an exciting opportunity for the development of Wnt inhibitors. Various compounds such as porcupine inhibitor[21] and tankyrase inhibitor[32] should be tested for the treatment of cancers containing RNF43 mutations.

METHODS SUMMARY

Cell culture, transfection, STF assays, immunoprecipitation and immunoblotting were performed as previously described[32,33]. Information on plasmid expression constructs is available on request.

Full Methods and any associated references are available in the online version of the paper at www.nature.com/nature.

Received 10 October 2011; accepted 6 March 2012.
Published online 29 April 2012.

1. Clevers, H. Wnt/β-catenin signaling in development and disease. *Cell* **127,** 469–480 (2006).
2. MacDonald, B. T., Tamai, K. & He, X. Wnt/β-catenin signaling: components, mechanisms, and diseases. *Dev. Cell* **17,** 9–26 (2009).
3. Simons, M. & Mlodzik, M. Planar cell polarity signaling: from fly development to human disease. *Annu. Rev. Genet.* **42,** 517–540 (2008).
4. Kazanskaya, O. *et al.* R-Spondin2 is a secreted activator of Wnt/β-catenin signaling and is required for *Xenopus* myogenesis. *Dev. Cell* **7,** 525–534 (2004).
5. Kim, K. A. *et al.* Mitogenic influence of human R-spondin1 on the intestinal epithelium. *Science* **309,** 1256–1259 (2005).
6. Kim, K. A. *et al.* R-Spondin family members regulate the Wnt pathway by a common mechanism. *Mol. Biol. Cell* **19,** 2588–2596 (2008).

7. Ohkawara, B., Glinka, A. & Niehrs, C. Rspo3 binds syndecan 4 and induces Wnt/PCP signaling via clathrin-mediated endocytosis to promote morphogenesis. *Dev. Cell* **20,** 303–314 (2011).
8. Aoki, M. *et al.* R-spondin3 is required for mouse placental development. *Dev. Biol.* **301,** 218–226 (2007).
9. Blaydon, D. C. *et al.* The gene encoding R-spondin 4 (*RSPO4*), a secreted protein implicated in Wnt signaling, is mutated in inherited anonychia. *Nature Genet.* **38,** 1245–1247 (2006).
10. Kazanskaya, O. *et al.* The Wnt signaling regulator R-spondin 3 promotes angioblast and vascular development. *Development* **135,** 3655–3664 (2008).
11. Parma, P. *et al.* R-spondin1 is essential in sex determination, skin differentiation and malignancy. *Nature Genet.* **38,** 1304–1309 (2006).
12. Sato, T. *et al.* Paneth cells constitute the niche for Lgr5 stem cells in intestinal crypts. *Nature* **469,** 415–418 (2011).
13. Ootani, A. *et al.* Sustained *in vitro* intestinal epithelial culture within a Wnt-dependent stem cell niche. *Nature Med.* **15,** 701–706 (2009).
14. Zhao, J. *et al.* R-Spondin1 protects mice from chemotherapy or radiation-induced oral mucositis through the canonical Wnt/β-catenin pathway. *Proc. Natl Acad. Sci. USA* **106,** 2331–2336 (2009).
15. Nam, J. S., Turcotte, T. J., Smith, P. F., Choi, S. & Yoon, J. K. Mouse cristin/R-spondin family proteins are novel ligands for the Frizzled 8 and LRP6 receptors and activate β-catenin-dependent gene expression. *J. Biol. Chem.* **281,** 13247–13257 (2006).
16. Wei, Q. *et al.* R-spondin1 is a high affinity ligand for LRP6 and induces LRP6 phosphorylation and β-catenin signaling. *J. Biol. Chem.* **282,** 15903–15911 (2007).
17. Binnerts, M. E. *et al.* R-Spondin1 regulates Wnt signaling by inhibiting internalization of LRP6. *Proc. Natl Acad. Sci. USA* **104,** 14700–14705 (2007).
18. Carmon, K. S., Gong, X., Lin, Q., Thomas, A. & Liu, Q. R-spondins function as ligands of the orphan receptors LGR4 and LGR5 to regulate Wnt/β-catenin signaling. *Proc. Natl Acad. Sci. USA* **108,** 11452–11457 (2011).
19. de Lau, W. *et al.* Lgr5 homologues associate with Wnt receptors and mediate R-spondin signalling. *Nature* **476,** 293–297 (2011).
20. Glinka, A. *et al.* LGR4 and LGR5 are R-spondin receptors mediating Wnt/b-catenin and Wnt/PCP signalling. *EMBO Rep.* **12,** 1055–1061 (2011).
21. Chen, B. *et al.* Small molecule-mediated disruption of Wnt-dependent signaling in tissue regeneration and cancer. *Nature Chem. Biol.* **5,** 100–107 (2009).
22. Gonzalez-Sancho, J. M., Brennan, K. R., Castelo-Soccio, L. A. & Brown, A. M. Wnt proteins induce dishevelled phosphorylation via an LRP5/6- independent mechanism, irrespective of their ability to stabilize beta-catenin. *Mol. Cell. Biol.* **24,** 4757–4768 (2004).
23. Gurney, A. L. Frizzled-binding agents and uses thereof. US patent 201037041 (2011).
24. Mukai, A. *et al.* Balanced ubiquitylation and deubiquitylation of Frizzled regulate cellular responsiveness to Wg/Wnt. *EMBO J.* **29,** 2114–2125 (2010).
25. Kim, C. H. *et al.* Repressor activity of Headless/Tcf3 is essential for vertebrate head formation. *Nature* **407,** 913–916 (2000).
26. Nasevicius, A. *et al.* Evidence for a frizzled-mediated wnt pathway required for zebrafish dorsal mesoderm formation. *Development* **125,** 4283–4292 (1998).
27. Smith, A. N., Miller, L. A., Song, N., Taketo, M. M. & Lang, R. A. The duality of β-catenin function: a requirement in lens morphogenesis and signaling suppression of lens fate in periocular ectoderm. *Dev. Biol.* **285,** 477–489 (2005).
28. Kreslova, J. *et al.* Abnormal lens morphogenesis and ectopic lens formation in the absence of β-catenin function. *Genesis* **45,** 157–168 (2007).
29. Machon, O. *et al.* Lens morphogenesis is dependent on Pax6-mediated inhibition of the canonical Wnt/β-catenin signaling in the lens surface ectoderm. *Genesis* **48,** 86–95 (2010).
30. Wang, J. *et al.* Dishevelled genes mediate a conserved mammalian PCP pathway to regulate convergent extension during neurulation. *Development* **133,** 1767–1778 (2006).
31. Wu, J. *et al.* Whole-exome sequencing of neoplastic cysts of the pancreas reveals recurrent mutations in components of ubiquitin-dependent pathways. *Proc. Natl Acad. Sci. USA* **108,** 21188–21193 (2011).
32. Huang, S. M. *et al.* Tankyrase inhibition stabilizes axin and antagonizes Wnt signalling. *Nature* **461,** 614–620 (2009).
33. Zhang, Y. *et al.* RNF146 is a poly(ADP-ribose)-directed E3 ligase that regulates axin degradation and Wnt signalling. *Nature Cell Biol.* **13,** 623–629 (2011).

Supplementary Information is linked to the online version of the paper at www.nature.com/nature.

Acknowledgements We thank G. Yu, T. Lewis, Q. Song, J. Garver, J. Wang, B. Lu, B. Guo, Q. Fang, X. Shi, J. Sprunger and R.Freeman for technical assistance, R.-F. Kwong and T. Fleming for generating ZNRF3 antibodies, K. Lee and J. Halupowski for mouse maintenance, and J. Tchorz, A. Jaffe, N. Kubica, M. Hild, J. Solomon, Y. Yang, J. Tchorz, E. Wiellette, G. Michaud, D. Cutis and K. Seuwen for comments and advice. We also thank S. Goto for providing FZD4 and FZD4 K0 plasmids.

Author Contributions H.-X.H. initiated the project, characterized the function of ZNRF3 in cultured cells and mice, and identified ZNRF3 antagonistic antibodies. H.-X.H. and Y.X. discovered the R-spondin and ZNRF3 link. Y.X. led mechanistic studies on R-spondin, LGR4 and ZNRF3. H.-X.H., Y.X., Y.Z., H.L., C.M., D.L., H.R., X.M., Q.M., T.B., P.M.F., M.W.K., J.A.P., F.C.S. and F.C. conceived and designed the study. H.-X.H., Y.X., Y.Z., O.C., E.O., M.A., H.L., C.M., D.L., H.R., X.M., Q.M., R.Z., F.C.S. and F.C. designed and implemented experiments. H.-X.H., Y.X., Y.Z. and F.C. wrote the manuscript.

Author Information Reprints and permissions information is available at www.nature.com/reprints. The authors declare no competing financial interests. Readers are welcome to comment on the online version of this article at www.nature.com/nature. Correspondence and requests for materials should be addressed to F.C. (feng.cong@novartis.com).

METHODS

Plasmids. Full-length human *ZNRF3* complementary DNA (NCBI accession number NM_001206998) was generated by fusing a short variant (NM_032173) and a synthesized 300-base-pair 5′ fragment. *ZNRF3* cDNA resistant to *ZNRF3*-1 siRNA was generated by two-step PCR and it was used as template for generating ZNRF3 ΔRING (missing amino acids 293–334) and ZNRF3 ECD-TM (missing amino acids 1–256). ZNRF3 was tagged with an N-terminal triple Myc epitope immediately after a signal peptide, or a C-terminal HA epitope. FZD8, FZD4 and FZD5 were tagged with an N-terminal triple Myc epitope right after the signal peptide. RSPO1 was fused with GFP at its C terminus. LGR4 was tagged with HA epitope at its C terminus. cDNAs are cloned in various mammalian expression vectors under control of the cytomegalovirus (CMV) promoter. Plasmids were sequenced to confirm the absence of undesirable mutations. Details of plasmids are available on request.

Cell culture, infection, transfection and RNA interference. HEK293 cells and its derivatives were grown in DMEM supplemented with 10% FBS. Various constructs were introduced into HEK293 or HEK293-STF cells through retroviral or lentiviral infection using standard protocols. Plasmid or siRNA transfection was done using FuGENE 6 (Roche) or Dharmafect 1 (Dharmacon), respectively. RSPO1, RSPO2, RSPO3 and RSPO4 were purchased from R&D Systems.

Sequences of siRNAs used are as follows: *ZNRF3-1* (QiagenSI03089744), sense, 5′-CCCAGUAUGAGACCAUGUATT-3′; antisense, 5′-UACAUGGUCUCAUACUGGGAG-3′. *ZNRF3-2* (Qiagen1027020), sense, 5′-GCUGCUACACUGAGGACUATT-3′; antisense, 5′-UAGUCCUCAGUGUAGCAGCCG-3′. *RNF43* (Dharmacon J-007004-09-0005), target sequence, 5′-GCAGAACAGAAAGCUAUUA-3′. *FZD6* (Dharmacon J-005505-07), target sequence, 5′-GAAGGAAGGAUUAGUCCAA-3′. *LGR4*-1 (Dharmacon J-003673-07), target sequence, 5′-AGGAUUCACUGUAACGUUA-3′ *LGR4*-2 (Dharmacon J-003673-08), target sequence, 5′-UUACUGAAGCGACGUGUUA-3′ *CTNNB1*, sense, 5′-UGUGGUCACCUGUGCAGCUdTdT-3′; antisense, 5′-AGCUGCACAGGUGACCACAdTdT-3′.

Luciferase assay. STF luciferase assays were performed using BrightGlo or DualGlo Luciferase Assay kits (Promega) according to the manufacturer's instructions.

Quantitative PCR with reverse transcription. Total RNA was extracted using the RNeasy Plus Mini Kit (Qiagen) and reverse transcribed with Taqman Reverse Transcription Reagents (Applied Biosystems) according to the manufacturer's instructions. The human colorectal cancer matched cDNA pair panel was purchased from Clontech. Transcript levels were assessed using the ABI PRISM 7900HT Sequence Detection System. Real-time PCR was performed in 12-μl reactions consisting of 0.6 μl of 20× Assay-on-Demand mix (premixed concentration of 18 μM for each primer and 5 μM for Taqman probe), 6 μl 2× Taqman Universal PCR Master Mix, and 5.4 μl diluted cDNA template. The thermocycling conditions used were 2 min at 50 °C, 10 min at 95 °C, followed by 40 cycles of 15 s at 95 °C and 1 min at 60 °C. All experiments were performed in quadruplicates. Gene expression analysis was performed using the comparative $\Delta\Delta C_T$ method with the housekeeping gene *GUSB* for normalization. The Assay-on-Demand reagents were purchased from Applied Biosystems.

Immunoblotting and immunoprecipitation. Immunoblotting and immunoprecipitation were performed as previously described[33]. Total cell lysates were prepared by lysing cells using RIPA buffer (50 mM Tris-HCl, pH 7.4, 150 mM NaCl, 1% NP-40, 0.5% sodium deoxycholate, 0.1% SDS and 1 mM EDTA) supplemented with protease inhibitors and phosphatase inhibitors, followed by centrifugation at 20,000*g* for 10 min at 4 °C. Equal amount of proteins were resolved by SDS–PAGE, transferred to nitrocellulose membranes, and incubated with primary antibodies overnight at 4 °C. Secondary antibodies conjugated with either horseradish peroxidise or infrared dyes were used for signal visualization by ECL film or LI-COR Odyssey scanner, respectively. Quantification of immunoblotting bands was performed by densitometric analysis with AlphaEaseFC software. For co-immunoprecipitation experiments, cells were lysed in buffer containing 50 mM Tris-HCl, pH 7.5, 150 mM NaCl, 1 mM EDTA, 0.8% Nonidet P40, phosphatase and protease inhibitors. Cleared cell lysates were incubated with the indicated antibodies and Protein G-sepharose beads (Amersham) overnight at 4 °C. Beads were washed four times with lysis buffer and the bound proteins were eluted in SDS sample buffer for immunoblotting analysis. The sources of primary antibodies are: anti-LRP6, anti-phospho-LRP6 (Ser 1490), anti-DVL2, anti-Myc tag, anti-GFP, anti-FZD6 (all Cell Signaling Technology); anti-IR-β, anti-Wnt3a (Abcam), anti-HA (Roche), anti-ZNRF3 (Santa Cruz), anti-β-catenin (BD Pharmingen) and anti-tubulin (Sigma).

Cell-based binding assay. HEK293 cells were transiently transfected with the indicated plasmids. Forty-eight hours after transfection, cells were incubated with RSPO1−GFP conditioned medium for 1 h. Cells were washed with PBS, fixed with 4% paraformaldehyde, incubated with anti-GFP and anti-Myc antibodies, stained with conjugated secondary antibodies and analysed by confocal fluorescence microscopy.

Solution-based binding assay. Conditioned medium of indicated proteins was mixed and incubated with Protein G beads overnight. Precipitates were washed extensively using buffer containing 50 mM Tris-HCl, pH 7.5, 150 mM NaCl, 1 mM EDTA, 0.8% Nonidet P40, and phosphatase and protease inhibitors. Bound proteins were eluted in SDS sample buffer, and subjected to immunoblotting analysis.

Cell-surface protein isolation. Cell-surface proteins were isolated by whole-cell biotinylation and avidin agarose pull-down using Cell Surface Protein Isolation Kit (Pierce) according to manufacturer's instructions.

Flow cytometric analysis. Cells were collected using trypsin-free cell dissociation buffer (Invitrogen) and resuspended in FACS buffer (PBS with 1% BSA and 0.02% sodium azide). After blocking, cells were incubated with anti-LRP6 (R&D system), anti-Myc-Alexa fluor 647 (Cell Signaling Technology) or anti-pan-frizzled (18R5) antibody for 1 h at 4 °C, followed by incubation with conjugated secondary antibodies where applicable. After extensive washes using FACS buffer, cells were stained with propidium iodide and subjected to multichannel analysis using a BD LSR II flow cytometer. Fluorescence signals from propidium-iodide-negative cells were displayed in histogram plots. Inducible heterodimerization of LGR4 and ZNRF3 was achieved using an iDimerize Heterodimerization Kit (Clontech) by fusing DmrC and DmrA to the C terminus of LGR4 and ZNRF3, respectively.

Pulse-chase experiment. For ^{35}S-labelling-based pulse-chase, cells were starved for 1 h at 37 °C in labelling medium (methionine-free and cysteine-free DMEM supplemented with 10% dialysed FBS), and 200 μCi of ^{35}S-labelled methionine and cysteine (Perkin Elmer) was added to each 10-cm plate. After 1 h of labelling, radioactive labelling medium was replaced with chase medium containing 100 μg ml^{-1} methionine and 500 μg ml^{-1} cysteine. Cells were treated with 50% Wnt3a conditioned media 3 h after pulse labelling. At the indicated time points, cells were lysed in RIPA buffer and cell lysates were immunoprecipitated using an anti-LRP6 antibody at 4 °C overnight. After extensive washes using RIPA buffer, immunoprecipitates were treated with lambda phosphotase (New England Biolabs) to remove phosphates from LRP6. Bound proteins were eluted in SDS sample buffer and resolved by SDS–PAGE, and analysed by autoradiography. For biotinylation-based pulse-chase, cells were washed and incubated with PBS containing sulfo-NHS-SS-biotin (Pierce) for 15 min at 37 °C. After terminating the cross-linking reaction using quenching solution, cells were washed, fed with fresh growth medium and returned to the 37 °C incubator. At the indicated time points, cells were lysed in RIPA buffer, and biotinylated proteins were isolated using avidin agarose and subjected to immunoblotting analysis.

Cellular ubiquitylation assay. The cellular ubiquitylation assay was performed as described previously[24]. HEK293 cells were co-transfected with Myc–FZD4, HA–ubiquitin, and ZNRF3, ZNRF3ΔRING or empty vector. Thirty-six hours after transfection, cells were treated with biotinylation agent and lysed in RIPA buffer with 5 mM *N*-ethyl maleimide. Biotinylated cell-surface proteins were isolated by avidin agarose and eluted by boiling for 10 min in SDS lysis buffer (1% SDS, 50 mM NaF and 1 mM EDTA) supplemented with 50 mM dithiothreitol (DTT). Eluates were diluted using RIPA buffer, and immunoprecipitated using anti-Myc antibodies. Immunoprecipitates were resolved by SDS–PAGE and analysed by immunoblotting assay. To examine the effect of ZNRF3 knockdown on frizzled ubiquitylation, HEK293 cells were transfected with control pGL2 siRNA or *ZNRF3* siRNA and 48 h later transfected again with Myc–FZD4 and HA–ubiquitin. To examine the effect of R-spondin on frizzled ubiquitylation, HEK293 cells were transfected with Myc–FZD4 and HA–ubiquitin, and treated with 500 ng ml^{-1} RSPO1 overnight.

***In vitro* autoubiquitylation assay.** Recombinant N-terminal glutathione *S*-transferase-tagged ZNRF3 intracellular domain (ICD) protein was produced in *Escherichia coli* and purified using glutathione-agarose beads. Next, 0.6 μM of ZNRF3 ICD was incubated with 125 nM E1 ubiquitin-activating enzyme, 2 μM E2 ubiquitin-conjugating enzyme and HA-ubiquitin (Boston Biochem) at 37 °C for 6 h in ubiquitylation buffer (50 mM Tris-HCl, pH 8.0, 100 mM NaCl, 5 mM $MgCl_2$-ATP and 1 mM DTT). Samples were resolved by SDS–PAGE and subjected to immunoblotting analysis.

Generation of human ZNRF3 antibody. The HuCAL GOLD phage-display library was used for selection of ZNRF3-specific Fab fragments. Fc–ZNRF3 ECD (amino acids 56–216) protein produced in HEK293FS cells (Invitrogen) was used for phage panning. Fab clones were screened by ELISA using Fc–ZNRF3 ECD, and their binding to ZNRF3 was verified by FACS analysis using HEK293 cells stably expressing ZNRF3 ΔRING.

Zebrafish and *Xenopus* experiments. Zebrafish were maintained using standard methods[34,35]. Experiments using *Xenopus* embryos were performed as described previously[36]. *In vitro* transcription was performed to synthesize capped mRNA

using linearized plasmids containing human ZNRF3, ZNRF3 ΔRING and GFP as a template using a mMESSAGE mMACHINE kit (Ambion). For zebrafish, 200 pg of human *ZNRF3* wild-type mRNA or 400 pg of ZNRF3 ΔRING mRNA was injected into the embryos at the 1–2-cell stage. For *Xenopus*, 200 pg of *ZNRF3* wild-type, ZNRF3 ΔRING or control GFP mRNA was injected into two blastomeres in 4-cell-stage embryos at the marginal zone. For whole-mount *in situ* hybridization, embryos at the indicated stages were fixed overnight in 4% paraformaldehyde, and stained with digoxigenin (DIG)-labelled antisense probes using standard protocols[34]. To analyse the expression of *Xenopus znrf3*, total RNA was extracted from embryos at different stages, and analysed by quantitative PCR with reverse transcription (qRT–PCR) using Applied Biosystems SYBR-Green Master Mix. The primers used were: *znrf3*, 5′-GATGGAGAGGAG CTGAGAGTCATTC-3′ (forward), 5′-GATAACTCGCTGTTGCTGCTG-3′ (reverse); H4 histone, 5′- CGGGATAACATTCAGGGTA-3′ (forward), 5′-TCCATGGCGGTAACTGTC-3′ (reverse). Samples were normalized against H4 histone as an internal control. For RT–PCR with *Xenopus* animal caps, mRNA was injected into the animal poles of both blastomeres at the 2-cell stage. The animal caps were isolated at stage 8.5 and cultured until stage 10.5 for RT–PCR. The primers used were: *siamois*, 5′-CTCCAGCCACCAGTACCAGATC-3′ (forward), 5′-GGGGAGAGTGGAAAGTGGTTG-3′ (reverse); *xnr3*, 5′-TCC ACTTGTGCAGTTCCACAG-3′ (forward), 5-ATCTCTTCATGGTGCCTCAGG-3′ (reverse), and *EF-1α* (also known as *eef1a1*), 5-CAGATTGGTGCTGGATATGC-3′ (forward), 5′-ACTGCCTTGATGACTCCTAG-3′ (reverse). Cell transplantation experiments were performed essentially as described[34]. In brief, donor embryos were injected with the *ZNRF3* or ZNRF3(ΔRING) mRNA and a 4% tetramethylrhodamine-dextran (10 kDa) solution. Small clones of cells were transplanted from donor embryos at the high-to-oblong stages to stage-matched wild-type hosts, and these were then individually tracked and photographed using fluorescence microscopy. Analysis of convergent extension movements by cell tracking was performed as previously described[37]. In brief, 1 nl of 10 kDa dextran-conjugated Alexa 488 lineage tracer (Invitrogen) was injected into the yolk just below the margin at the 256-cell stage. The embryos were observed for cell movements towards the midline of the embryo and extensions along the anterior–posterior axis. Live images were taken at 30% epiboly, shield and 75% epiboly stages of the same embryos.

Generation and characterization of *Znrf3*-deficient mice. In the targeting vector, exon 7 encoding the RING domain is flanked by two *loxP* sites. Linearized targeting vector was electroporated into 129/SvJ embryonic stem (ES) cells, and G418-resistant ES clones were first screened by nested PCR, and then subjected to Southern blot analysis. Genomic DNA was digested with XmnI or BglII restriction enzymes, and hybridized with probes positioned outside the 5′ and 3′ homologous regions, respectively (Supplementary Fig. 13). ES clone 5A7 was used for blastocyst injection and chimaeric males were mated with Cre-deleter mice in the C57BL/6J background. F_1 mice with Cre-mediated deletion of exon 7 were identified by PCR, and further backcrossed in the C57BL/6J background. Wild-type, heterozygous and homozygous mice were identified by 'multiplex' PCR with the following three primers: forward primer 1, 5′-TATCATGGTCTGTATACCGGGATCG-3′; forward primer 2, 5′-CATACT TTGGGCTCATGAGCAAGC-3′; reverse primer, 5′- GCAGGTATACATTAC CACACCC-3′. Deletion of the RING domain of mouse Znrf3 creates a frameshift and premature termination. Truncated *Znrf3* transcript was not detected by qPCR assay in *Znrf3* knockout samples, so it is presumably degraded by nonsense-mediated mRNA decay. $Znrf3^{-/-}$ mouse embryos and wild-type littermate controls were generated by timed mating of heterozygous parents. At the indicated embryonic stage, pregnant females were euthanized and embryos were dissected out for imaging or histology analysis after fixation in 4% paraformaldehyde overnight at 4 °C. After dehydration in gradient serials of ethanol, the embryo was paraffin-embedded on head for horizontal sectioning, and slides were stained by haematoxylin and eosin. Whole mount *in situ* hybridization with E9.5 mouse embryos was carried out according to standard protocols using 25 nM double DIG-labelled locked nucleic acid probe from Exiqon. The mouse *Axin2* probe sequence was 5′-TCTCTAACATCCACTGCCAGA-3′. For the LacZ staining experiment, Znrf3 heterozygous males carrying the *Axin2*-LacZ transgene were mated with Znrf3 heterozygous females to generate E9.5 and E10.5 mouse embryos. Embryos were freeze-sectioned after fixation and cryopreservation in sucrose gradient. Frozen sections were stained with Tissue Stain Base Solution containing X-Gal (Millipore), post-fixed in 4% paraformaldehyde and counterstained with 0.005% nuclear fast red. Primers for *Axin2*-LacZ genotyping were: 5′-AAGAAGAAGAGGAAGGTGGAAGATCCCGTCGTTTTAC-3′ (forward), 5′-GAGACGTCACGGAAAATGCCGCTCATC-3′ (reverse).

Statistical analysis. Results are expressed as mean ± s.d. from an appropriate number of experiments as indicated in the figure legends.

34. Nusslein-Volhard, C. & Dahm, R. *Zebrafish. A Practical Approach.* (Oxford Univ. Press, 2002).
35. Westerfield, M. *The Zebrafish Book: a Guide for the Laboratory Use of Zebrafish (*Brachydanio rerio*).* (Univ. Oregon Press, 1995).
36. Goentoro, L. & Kirschner, M. W. Evidence that fold-change, and not absolute level, of β-catenin dictates Wnt signaling. *Mol. Cell* **36,** 872–884 (2009).
37. Gerdes, J. M. *et al.* Disruption of the basal body compromises proteasomal function and perturbs intracellular Wnt response. *Nature Genet.* **39,** 1350–1360 (2007).